# Production Rate of SiO Gas from Industrial Quartz and Silicon

CAROLINE SINDLAND and MERETE TANGSTAD

The production rate of SiO gas from industrial quartz and silicon has been investigated by isothermal heat treatment experiments. Mixtures of silicon and different quartz samples have been heated to temperatures ranging from 1650 °C to 1950 °C and held for 30 to 120 minutes before cooling. The weight loss of each sample has been correlated to degree of reaction and a model for the reaction rate of Si + $SiO_2$ has been developed based on these values. Five different types of industrial quartz were used in the experiments. No significant difference was found in their reaction rate, even though there are large variations in impurity content, melting rate, decrepitation, and phase transformation rate of each sample. Further on, it is shown that the reaction rate of silicon mixed with various types of quartz can be described by an Arrhenius equation: $d\alpha/dt = k_0\,A\exp(-Q/RT)$. A reaction constant ($k_0$) equal to $6.25\,10^8\,\mathrm{g\,s^{-1}\,m^{-2}}$ and an activation energy ($Q$) equal to $557\,\mathrm{kJ\,mol^{-1}}$ were obtained by linear regression. The degree of reaction ($\alpha$) is shown to be increasing with available reaction area, temperature, and time.

## I. INTRODUCTION

SILICON is produced in Norway by the use of submerged arch furnaces (SAF) with coal, charcoal, woodchips, quartz, and electricity as input and silicon, $CO_g$, and silica as output. Reduction of quartz to form silicon occurs in several intermediate steps and the process is thoroughly described in Production of High Silicon Alloys by Schei et al.[1] A high silicon yield is one of the main goals in silicon production and it is dependent on the amount of losses in form of $SiO_g$ escaping through the exhaust, SiC build up in the furnace, and silicon metal lost during tapping. The first one, the amount of $SiO_g$ escaping through the exhaust, is dependent on the amount of $SiO_g$ produced in a silicon furnace. Investigation of the $SiO_g$-producing reactions is hence one step towards a more controlled silicon yield.

There are two $SiO_g$ forming reactions within a silicon furnace: the reaction between silicon carbide and silica and the reaction between silicon and silica. The incomplete reduction of silica with carbon ($SiO_2 + C = CO + SiO$) can be divided into two steps: formation of silicon carbide and reaction between silicon carbide and silica to form SiO gas. The last step, reaction between silica and silicon carbide, is shown to be the rate determining step and the overall reaction is therefore not considered in this article.[2] The first reaction, the reaction between silica and silicon carbide, has been investigated by Tangstad et al., who developed a model for the reaction rate, including a reaction constant and activation energy.[3] The other reaction has not been thoroughly investigated and no model for reaction rate has been found in the literature. The goal of this project is hence to investigate the reaction rate of silicon and silica mixtures, described by Eq. [1], and to develop a model describing the reaction rate as function of temperature, time, available reaction area, and quartz quality. This will make it possible to compare the two $SiO_g$-producing reactions and further on give a better understanding of total $SiO_g$ losses in a silicon furnace.

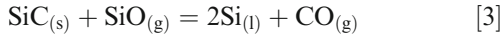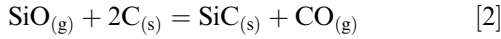$$SiO_{2(s,l)} + Si_{(l)} = 2SiO_{(g)} \qquad [1]$$

### A. Metallurgical Production of High-Silicon Alloys

The silicon furnace is normally divided in two zones: a low-temperature upper zone with temperatures ranging from 1300 °C to 1900 °C and a hot lower zone close to 2000 °C. Quartz and carbon materials are added to the top of a silicon furnace. Carbon will react in the low-temperature zone according to Eq. [2] and silicon and silica will be formed in the low-temperature zone from the condensation reaction given by the reverse of Eq. [1]. The inputs in the hot zone are therefore $SiO_2$, C, SiC, and Si. The main silicon-producing reaction is

CAROLINE SINDLAND and MERETE TANGSTAD are with the The Department of Materials Science and Engineering, Norwegian University of Science and Technology, 7491 Trondheim, Norway. Contact e-mail: merete.tangstad@ntnu.no

happening within the hot zone and is given by Eq. [3]. The source of SiO gas is reaction between silicon and silica as well as silica and silicon carbide, according to Eqs. [1] and [4]. The CO gas formed in the hot-temperature zone and any SiO that does not react according to Eq. [3] will rise to the low-temperature zone. Some of the rising SiO gas will condensate according to the reverse of Eq. [1], while the rest will rise further and oxidize before it leaves the furnace as $SiO_2$ in the exhaust system. The silica can be collected from the off gas and sold as a valuable product, but the goal is to control the amount of silica in the off gas, regardless of its value.

$$SiO_{(g)} + 2C_{(s)} = SiC_{(s)} + CO_{(g)} \qquad [2]$$

$$SiC_{(s)} + SiO_{(g)} = 2Si_{(l)} + CO_{(g)} \qquad [3]$$

$$2SiO_{2(s,l)} + SiC_{(s)} = 3SiO_{(g)} + CO_{(g)} \qquad [4]$$

### B. Thermodynamics of the Si-O-C System

There are multiple possible reactions in a Si-O-C system. The stability of reactions including $SiO_g$ is plotted as function of temperature and SiO pressure in Figure 1, where the total pressure of the system is assumed to be 1 bar $= P_{SiO} + P_{CO}$. Silicon and silica react to form SiO gas at SiO pressures below 0.1 bar when the temperature is 1600 °C, at pressures below 0.6 bar when the temperature is 1800 °C and at any pressure when temperature is

increased above 1850 °C. The standard Gibbs free energy for the reactions (given in kJ) is listed in Table I for temperatures ranging from 1400 to 2000 °C.

### C. The Reaction Rate of Silicon and Silica

The rate of reaction between silicon and silica in pellets, described by Eq. [1], increases from 1550 °C to its maximum at 1850 °C, according to Bao et al.[4] The reaction rate decreases at higher temperatures and two possible reasons are given: the reaction between silica and silicon is exothermic and the Si vapor increases at higher temperatures, leaving a very low reaction area between $SiO_2$ and Si. The reaction rate of silicon/silica pellets was calculated to be higher than the one of silica/SiC pellets at temperatures below 1820 °C and the opposite was measured for temperatures above 1820 °C. The difference at high temperatures was assumed to be due to a low silicon/silica reaction rate.

Andersen reported an exponential increase of reaction rate from 1450 °C to 1723 °C, a reduced reaction rate from 1723 °C to 1860 °C and finally a significant increase of reaction rate at 1910 °C.[5] Formation of bubbles at the silicon/silica interface was observed during heating of silicon and silica pellets between 1750 °C and 1869 °C in a wettability furnace, indicating formation of SiO gas. The drop in reaction rate at these temperatures was therefore related to a high viscosity of the liquid silica and a low gas removal rate. The equilibrium pressure of SiO gas exceeds 1 bar around 1860 °C and this is pointed out as a possible reason for
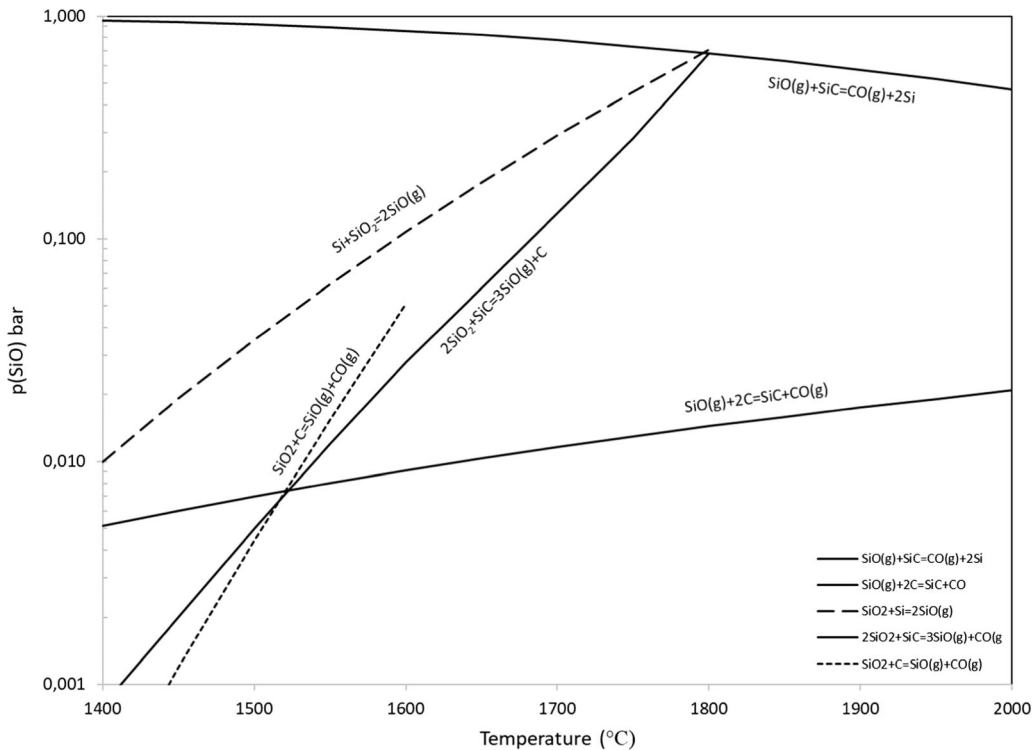


Fig. 1—Equilibrium pressure of reactions within the Si-C-O system, calculated by the use of HSC Chemistry 9.

## Table I. The Standard Gibbs Free Energy [kJ] for Reactions Within the Si-C-O System

| Temp. °C | $SiO_{(g)} + SiC = Co_{(g)} + 2Si$ [kJ] | $SiO_2 + Si = 2SiO_{(g)}$ [kJ] | $2SiO_2 + SiC = 3SiO_{(g)} + CO_{(g)}$ [kJ] | $SiO_2 + SiC = SiO_{(g)} + CO_{(g)}$ [kJ] | $SiO_{(g)} + 2C = SiC + CO_{(g)}$ [kJ] | $SiO_2 + 3C = SiC + 2CO_{(g)}$ [kJ] | $Si + C = SiC$ [kJ] |
|---|---|---|---|---|---|---|---|
| 1400 | 42.78 | 128.25 | 299.28 | 113.05 | − 73.18 | 39.87 | − 57.98 |
| 1500 | 35.87 | 98.61 | 233.09 | 80.00 | − 73.09 | 6.92 | − 54.48 |
| 1600 | 28.25 | 69.47 | 167.20 | 47.10 | − 73.00 | − 25.90 | − 50.63 |
| 1700 | 20.63 | 40.48 | 101.59 | 14.34 | − 72.92 | − 58.58 | − 46.77 |
| 1800 | 13.00 | 12.01 | 37.02 | − 17.91 | − 72.85 | − 90.75 | − 42.92 |
| 1900 | 5.36 | − 16.18 | − 26.99 | − 49.89 | − 72.78 | − 122.67 | − 39.07 |
| 2000 | − 2.27 | − 55.20 | − 90.68 | − 81.70 | − 72.73 | − 154.43 | − 35.23 |

## Table II. Reaction Constant and Activation Energy for $2SiO_2 + SiC = 3SiO + CO$, Measured in Pellets.[3] $k_0$ is Given for the Case Where the Surface Area of $SiO_2$ is Limiting

| $k_0$ [g s$^{-1}$ cm$^{-2}$] | Q [kJ mol$^{-1}$] |
|---|---|
| $1.9 \times 10^5$ | 424-464 |

the increasing reaction rate at high temperatures. An activation energy between 438 kJ/mole and 528 kJ/mole is reported by Andersen.[5]

### D. Reaction Rate of Silica and Silicon Carbide

The second reaction producing SiO gas in the silicon furnace (in addition to Si/SiO$_2$ reaction) is described by Reaction 4 where SiO$_2$ reacts with SiC to SiO and CO gas. The reaction rate of the reaction between SiC and silica has been measured by Tangstad et al., describing the rate by Eq. [5], under the assumption that the surface area of SiO$_2$ is rate limiting.[3] Their obtained values for reaction constant and activation energy are presented in Table II. The measurements were done on pellets which give a high reaction area compared to experiments with particles. They did not find any significant difference between pellets of quartz and SiC compared to pellets of cristobalite and SiC.

$$\frac{d\alpha}{dt} = k_0 A_0 (1 - \alpha) \exp\left(\frac{-Q}{RT}\right), \qquad [5]$$

where $\alpha$ is the degree of reaction [ ], $t$ is the time [s], $k_0$ is the reaction constant $[g\,s^{-1}\,cm^{-2}]$, $A_0$ is the initial reaction area $[cm^2\,g^{-1}]$, $Q$ is the activation energy $[J\,mol^{-1}]$, $R[mol\,J^{-1}\,K^{-1}]$ is the gas constant, and $T$ is the temperature [K].

The reaction rate of silica and silicon carbide pellets has also been investigated by Bao et al. at an earlier stage.[4] They heated pellets of silica and silicon carbide to 1550, 1730, and 1820 °C at a heating rate of 15 °C/min and held it for a given time. They found that the reaction rate is almost constant at 1550 °C and then increases exponentially to 1820 °C, until the samples are almost completely consumed. Temperature accelerates the reaction substantially. Andersen found that the reaction rate increases exponentially from 1450 °C to about 1700 °C; it had a constant or reduced rate during melting and a rapid increase from 1770 °C.[5]

### E. Quartz

Quartz goes through multiple phase transitions when heated from room temperature to 1800 °C. The stable phase at room temperature is $\alpha$ - quartz which will transform into $\beta$ - quartz at 573 °C. Transition into HP-tridymite occurs at 870 °C before it is transformed into $\beta$ - cristobalite at 1470 °C and melting occurs at 1728 °C, according to Manual of Mineralogy.([6], p. 530) Melting occurs at 1713 °C according to SI-chemical data.[7] The transformation to tridymite as described in Manual of Mineralogy is debated in several other publications.[8–10] It is shown that tridymite is an impurity-derived structure

and not stable in pure silica. Transition from quartz to cristobalite seems to occur via a non-crystalline transition phase and can be described by Reaction 6.

$$Quartz \rightarrow Amorphous phase \rightarrow cristobalite \quad [6]$$
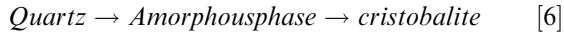
Phase transformation in different industrial quartz samples has been investigated by Jusnes and among them are the samples labeled quartz B, C, and D, later discussed in this article.[9] There is a significant difference in their transformation rate. The phase compositions of quartz B, C, and D after they have been heated to 1650 °C and held for 0, 30, and 60 minutes are presented in Figure 2. Quartz B has a higher rate of transformation than quartz C which again has a higher rate than quartz D.

Melting and decrepitation of silica have been investigated by Nordnes and Jusnes et al., and both properties seem to vary significant between different types of industrial quartz.[11, 12] A low amount of particles below 10 mm (< 5 pct) was found after shock heating of quartz C, while the amount of particles below 10 mm was about 30 pct for quartz B and about 75 pct for quartz D. There is also a significant difference in the melting rate of quartz B and C but no information has been obtained for the other samples used in this article. A summary of values obtained for melting and decrepitation of the quartz samples used in this article can be found in Figure 3.

### F. Wettability in the Si-O-C System

Silicon on graphite has an initial contact angle of about 120 °C, but liquid silicon will eventually wet the substrate due to formation of a SiC layer at the interface. The equilibrium contact angle of silicon on a graphite substrate is reported to be 3 to 40 °C by Ciftja et al and Dezellus et al.[13,14] The final angle is dependent on the surface roughness and is obtained after 5 to 10 min of heating.[13]

Silicon has a contact angle of 90 deg on solid silica substrates.[15] It has been observed that silicon droplets vibrate on silica substrates, resulting in an oscillating contact angle and further on spreading due to changes in the solid–liquid surface tension. An apparent average wetting angle between 90 deg and 95 deg is reported by other sources that also observed vibration of the silicon droplet where experiments were performed in 1 atm Ar atmosphere.[16,17] Formation and release of $SiO_g$ is a suggested cause of vibration and no secondary phase was found on the silicon/silica interface. Leakage paths like dimples and grooves are found to reduce the amount of vibration and a more constant wetting angle was observed in this case compared to heating on a smooth substrate.[16]

Heating of brown condensate in a sessile drop furnace has been performed by Vangskåsen.[18] The condensate consisted mostly of silicon and silica, products from the condensation of $SiO_g$, represented by Reaction 1 reversed. The silicon in the brown condensate melted away from the surrounding $SiO_2$ at temperatures above 1395 °C. The separation of silicon happened most

rapidly above 1700 °C. The remaining amorphous $SiO_2$ retained its shape up to the maximum temperature of the furnace at about 1850 °C and showed no signs of melting. Silicon and silica did not wet each other.

Images from melting and softening experiments performed with silica on a graphite substrate in a sessile drop furnace show a contact angle above 90 deg, meaning that the silica does not wet the graphite substrate.[11]

Boron nitride (BN) is one of the very few materials that is non-wetted by liquid silicon. The contact angle between the two materials has been reported to be between 105 and 145 deg, all within the non-wetting area.[19–21]

## II. EXPERIMENTAL

The reaction rate of five different quartz samples mixed with one type of metallurgical grade silicon has been investigated. Isothermal heat treatment of 1:1 molar mixtures of silicon and silica in graphite crucibles has been performed, to measure the weight loss after experiment as function of time and temperature, which have been correlated to reaction rate. A total of 30 experiments have been performed at temperatures between 1650 °C and 1950 °C, with holding times between 30 and 120 minutes and a heating rate of 50 K/min until isothermal temperature was reached. 17 of the experiments were performed with one type of quartz (quartz A) mixed with silicon of metallurgical grade, while another 13 experiments have been performed with four different industrial quartz samples (B to E), to investigate the effect of quartz type on the reaction rate of silicon and silica. Different size fractions of quartz E were heated, to investigate the effect of size fraction on the reaction rate. Both mixing and layering of the raw materials (with silicon on top of silica) were tested for experiments with quartz A. Mixing of the raw materials was the chosen method for the rest of the experiments. The chemical composition of the silicon was similar in all experiments but the size fraction of the silicon was equal to the size fraction of the quartz used in each experiment. Chemical composition and particle size of the silicon and quartz used in the experiments are presented in Tables III and IV, respectively. A list of all of the experiments, including quartz sample, size fraction, mixing/layering of raw materials, time, and temperature can be found in Table V.

A total of 20 g silicon and silica (1:1 molar ratio) was heated in high-density graphite crucibles, except experiment 5 where a h-BN crucible was used. 24 of the samples were heated in a resistance heat furnace, while 6 of the samples (experiment number 3, 4, 9, 10, 12, and 15) were heated in an induction heat furnace. All of the samples were inserted in a reaction chamber made of graphite, closed by a condensation chamber filled with SiC particles, as seen in Figure 4. A temperature gradient in the system causes any formed SiO gas that rises to condense on the SiC particles before the gas escape through the exhaust system of the furnace. The reaction chamber was vacuumed before it was filled with
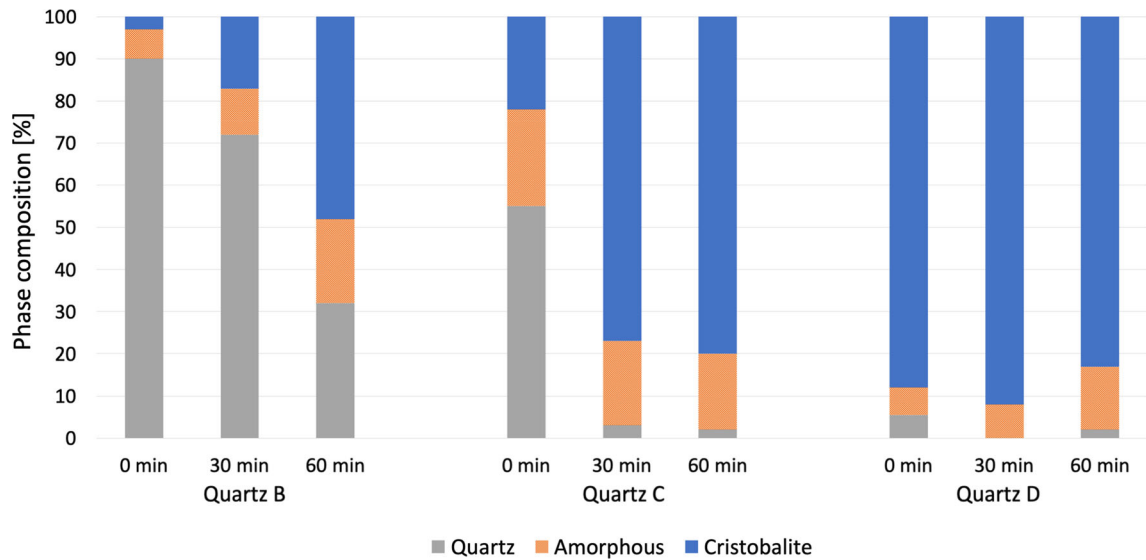
Fig. 2—Phase transformation in quartz B, C, and D after heating to 1600 °C for 0, 30, and 60 min obtained from work done by Jusnes.[9]
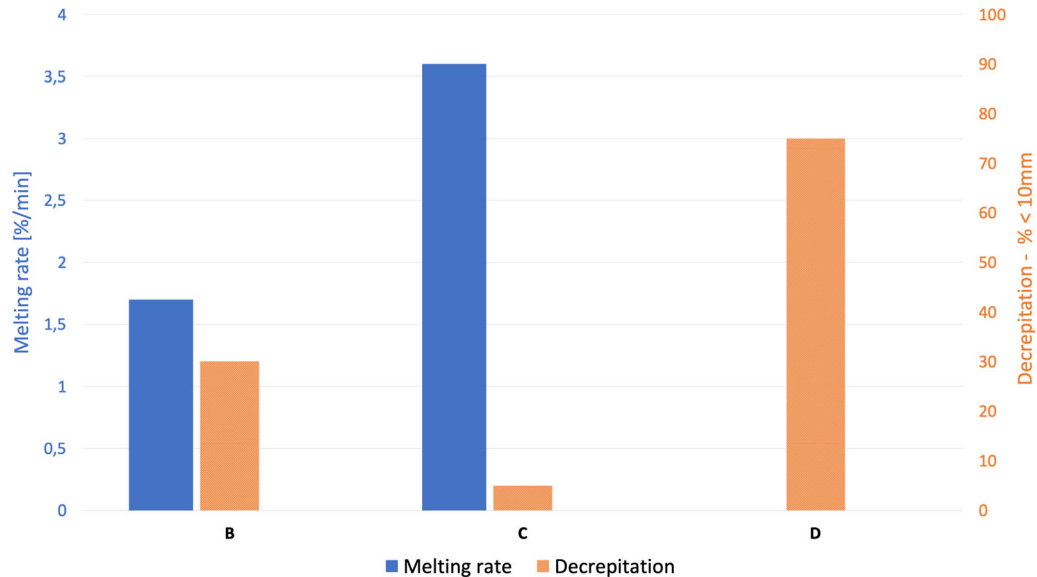


Fig. 3—Melting rate of quartz B and C at 1750 °C obtained from work done by Nordnes.[11] Decrepitation of quartz B, C, and D after shock heating to 1500 °C obtained from work done by Jusnes, given as percentage of particles that are below 10 mm.[12]

argon (99.999 pct) and heating started once a pressure of 1.5 bar was reached. A constant pressure of 1.5 bar was maintained by a flow of argon entering the top of the reaction chamber. The temperature was monitored by a C-type thermocouple covered by graphite, placed in the center of the sample crucible. The weight of the crucible was measured with and without sample before heating and with sample after heating, giving the total weight loss relatively to initial sample weight, described by Eq. [7].

$$Wt.loss = \frac{(\text{crucible, sample and } cover)_{\text{before}} - (\text{crucible, sample and cover})_{\text{after}}}{\text{sample weight before}}.$$

[7]

Wettability of silicon on silica was measured in a sessile drop furnace by heating of silicon on a substrate of different quartz samples in argon atmosphere, while images of the sample is taken thought the entire experiment. All of the samples were heated in the same furnace (furnace 1) except one parallel (with quartz C as substrate) that was heated in furnace 2. It would have been preferred to run multiple parallels in both furnaces but this was not possible due to technical problems with furnace 2. The images were analyzed and a wetting angle was obtained for each sample by the use of ImageJ. Substrates of quartz B to E were made by cutting and grinding of discs from core samples (a core sample of quartz A was not

**Table III. Composition and Size Fraction of the Silicon**

| Particle size (mm) | Si (Weight Percent) | Fe (Weight Percent) | Ca (Weight Percent) | Ti (ppmw) | P (ppmw) |
|---|---|---|---|---|---|
| 1 to 2, 2 to 5 and 5 to 8 | min 99.0 | max 0.40 | max 0.10 | 200 to 300 | 20 to 40 |

**Table IV. Composition and Size Fraction of the Quartz. Sample A was Analyzed by ICP-OES, While B to E was Analyzed by XRF. The Rest of the Sample is Assumed to be $SiO_2$**

| Name | Particle size (mm) | Al (Weight Percent) | Fe (Weight Percent) | K (Weight Percent) | Ca (Weight Percent) | Ti (Weight Percent) | Mg (Weight Percent) | Na (Weight Percent) | P (Weight Percent) |
|---|---|---|---|---|---|---|---|---|---|
| A | 2 to 5 | 0.031 | 0.012 | 0.009 | 0.0046 | 0.002 | 0.0017 | 0.001 | 0.0003 |
| B | 1 to 2 | 0.006 | 0.006 | 0.002 | < 0.0011 | < 0.001 | 0.0005 | < 0.0011 | < 0.0004 |
| C | 1 to 2 | 0.211 | 0.192 | 0.063 | 0.0026 | 0.017 | < 0.0005 | 0.0022 | 0.0016 |
| D | 1 to 2 | 0.038 | 0.010 | 0.017 | 0.0415 | 0.001 | < 0.0005 | 0.0125 | < 0.0004 |
| E | 1 to 2, 2 to 5 and 5 to 8 | 0.505 | 0.111 | 0.126 | 0.0324 | 0.016 | 0.0071 | 0.027* | 0.0016 |

*Above calibration limit and must be seen as guidance.

**Table V. Experiment Number, Quartz Type, Fraction, Temperature, Whether the Raw Materials Were Mixed or Layered, and Holding Time for Each Experiment are Listed as Well as sample Weight Loss After Heating**

| Exp. Nr | Quartz | Frac. [mm] | T [°C] | $t_{hold}$ [min] | Weight Loss [Weight Percent] | Raw Materials |
|---|---|---|---|---|---|---|
| 1 | blank | — | 1800 | 60 | ~ 0 | — |
| 2 | A | 2 to 5 | 1670 | 120 | 3.25 | mixed |
| 3 | A | 2 to 5 | 1655 | 120 | 2.50 | layered |
| 4 | A | 2 to 5 | 1750 | 60 | 3.49 | layered |
| 5 | A | 2 to 5 | 1750 | 60 | 4.40 | layered |
| 6 | A | 2 to 5 | 1775 | 120 | 12.65 | mixed |
| 7 | A | 2 to 5 | 1756 | 120 | 7.31 | layered |
| 8 | A | 2 to 5 | 1751 | 120 | 9.25 | mixed |
| 9 | A | 2 to 5 | 1750 | 180 | 8.95 | layered |
| 10 | A | 2 to 5 | 1850 | 30 | 9.08 | layered |
| 11 | A | 2 to 5 | 1880 | 60 | 22.00 | mixed |
| 12 | A | 2 to 5 | 1850 | 60 | 19.35 | layered |
| 13 | A | 2 to 5 | 1856 | 60 | 13.81 | layered |
| 14 | A | 2 to 5 | 1854 | 60 | 16.52 | mixed |
| 15 | A | 2 to 5 | 1850 | 120 | 32.10 | layered |
| 16 | A | 2 to 5 | 1932 | 30 | 46.63 | mixed |
| 17 | A | 2 to 5 | 1985 | 60 | 71.80 | mixed |
| 18 | A | 2 to 5 | 1959 | 60 | 55.52 | mixed |
| 19 | B | 1 to 2 | 1650 | 120 | 4.40 | mixed |
| 20 | B | 1 to 2 | 1850 | 60 | 20.56 | mixed |
| 21 | C | 1 to 2 | 1650 | 120 | 5.10 | mixed |
| 22 | C | 1 to 2 | 1750 | 120 | 11.83 | mixed |
| 23 | C | 1 to 2 | 1850 | 60 | 26.45 | mixed |
| 24 | C | 1 to 2 | 1950 | 30 | 47.35 | mixed |
| 25 | D | 1 to 2 | 1650 | 120 | 5.66 | mixed |
| 26 | D | 1 to 2 | 1850 | 60 | 23.20 | mixed |
| 27 | E | 1 to 2 | 1650 | 120 | 4.45 | mixed |
| 28 | E | 1 to 2 | 1850 | 60 | 22.57 | mixed |
| 29 | E | 2 to 5 | 1850 | 60 | 17.85 | mixed |
| 30 | E | 5 to 8 | 1650 | 120 | 2.60 | mixed |
| 31 | E | 5 to 8 | 1850 | 60 | 13.54 | mixed |

Each sample was weighted to 20.0 g prior to heating with a Si:$SiO_2$ molar ratio of 1:1 and heated in a graphite crucible except experiment 5 where a h-BN crucible was used.
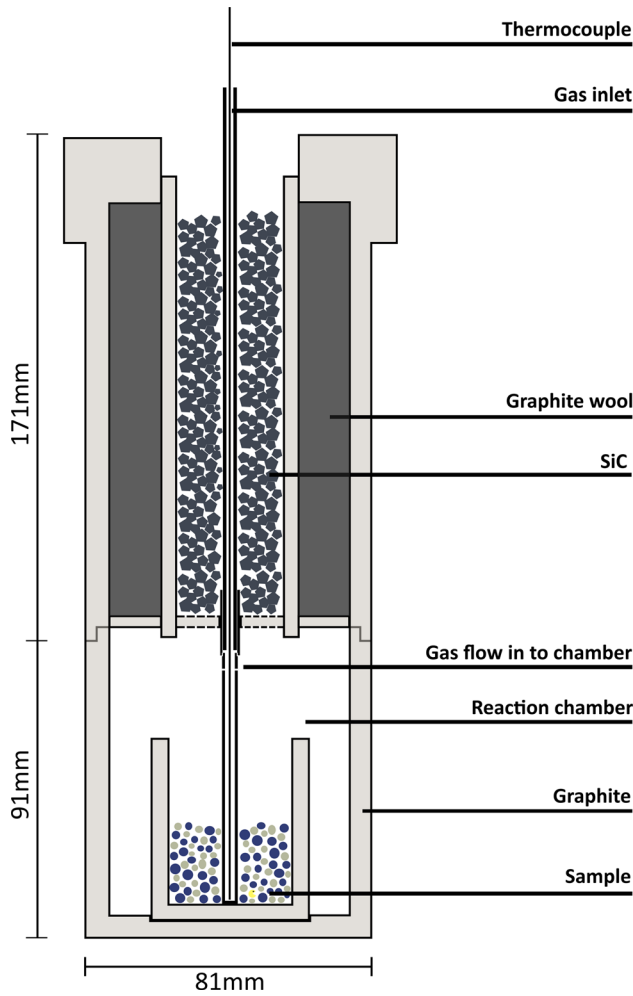
Fig. 4—Experimental setup.

available and the wettability of this sample was therefore not tested). The sample was set to be heated to 900 °C within 3 minutes before it was heated to 1350 °C at a heating rate of 50 K/min and finally at a rate of 5 K/min to 1523 °C. It was then set to be held at 1523 °C for 120 minutes before cooling. Pictures were taken throughout the entire experiment with 1 image per K (2 images per K during heating from 900 °C to 1450 °C).

## III. RESULTS AND DISCUSSION

Reaction rate of silicon and silica is both dependent on and increased by available reaction area, temperature, and time. This have been confirmed by 30 experiments where a mixture of silicon and different types of industrial quartz samples have been heated at temperatures ranging from 1650 °C to 1950 °C and times varying from 30 to 120 minutes. The degree of reaction is calculated based on weight loss of each sample and no significant difference between the reaction rate of the different types of industrial quartz was found, which will be further discussed in Section "III−A". The phase distribution after heating of the samples has been investigated by macro and SEM images and the properties of the different quartz samples are discussed, based on chemical analysis, XRD, and information on each specific sample found in the literature. A comparison of the two SiO-producing reactions in a silicon furnace and their behavior as a function of temperature will be discussed in Section "III−E", based on the result of this report and literature on the silica/SiC reaction rate.
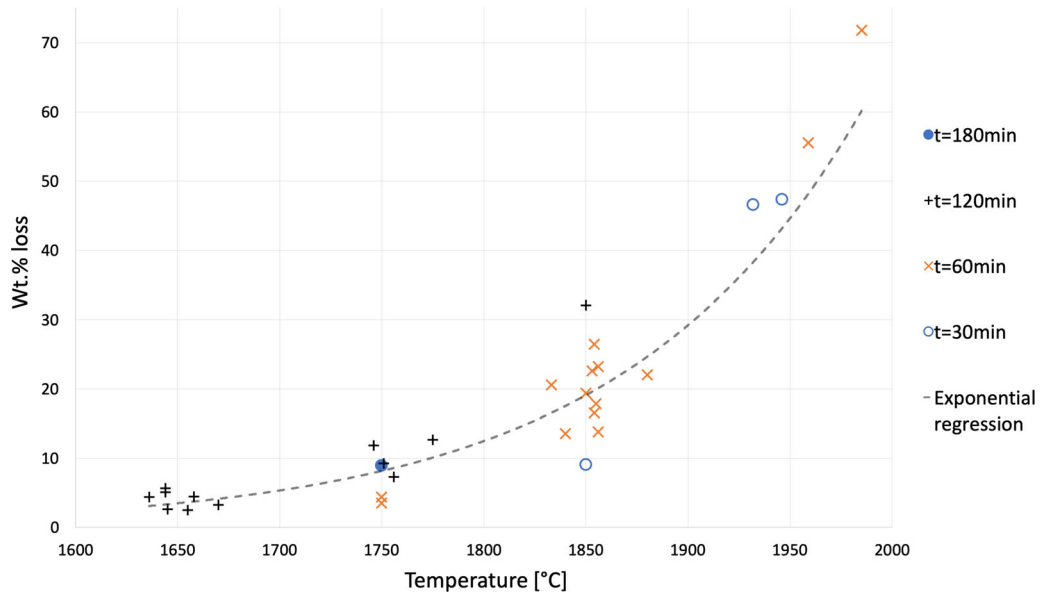


Fig. 5—The weight loss after heating samples of quartz A to E mixed with silicon. The dotted line is a regression (not the reaction rate model) based on all of the experimental data to indicate that weight loss increase with time and temperature.

The weight loss of each sample is listed in Table V and plotted as function of temperature in Figure 5. The weight loss increases with time and temperature, as indicated by a regression based on the data in Figure 5. It is assumed that the weight loss of a sample can be directly correlated to the reaction rate and the weight loss is assumed to be due to SiO formation only. This

will be discussed and justified in Section "III−B" section. Based on that, the reaction rate of silicon and silica mixtures was found to follow an Arrhenius equation, described by Eqs. [8] through [11] (where $\alpha$ is the degree of reaction [ ], $t$ [s] is the time, $k_0$ is the reaction constant [g s$^{-1}$ cm$^{-2}$], $A$ is the available reaction area [cm$^2$ g$^{-1}$], $A_{0,Si}$ is the initial reaction area of silicon [cm$^2$ g$^{-1}$], $r_{0,Si}$ is the initial radius of silicon particles, $F$ is the agglomeration factor, $Q$ is the activation energy [J], $\rho_{Si}$ is the density of silicon, $S_{part}$ and $V_{part}$ are the surface and volume of one silicon particle). There is no significant difference between the reaction rate of the five different quartz types. Values for reaction constant ($k_0$) and activation energy ($Q$) are presented in Table VI. The values have been obtained from the linear regression in Figure 6, an Arrhenius plot of all 30 samples.

**Table VI.   Values for Reaction Constant and Activation Energy Obtained from a Linear Regression in the Arrhenius Plot in Fig. 6**

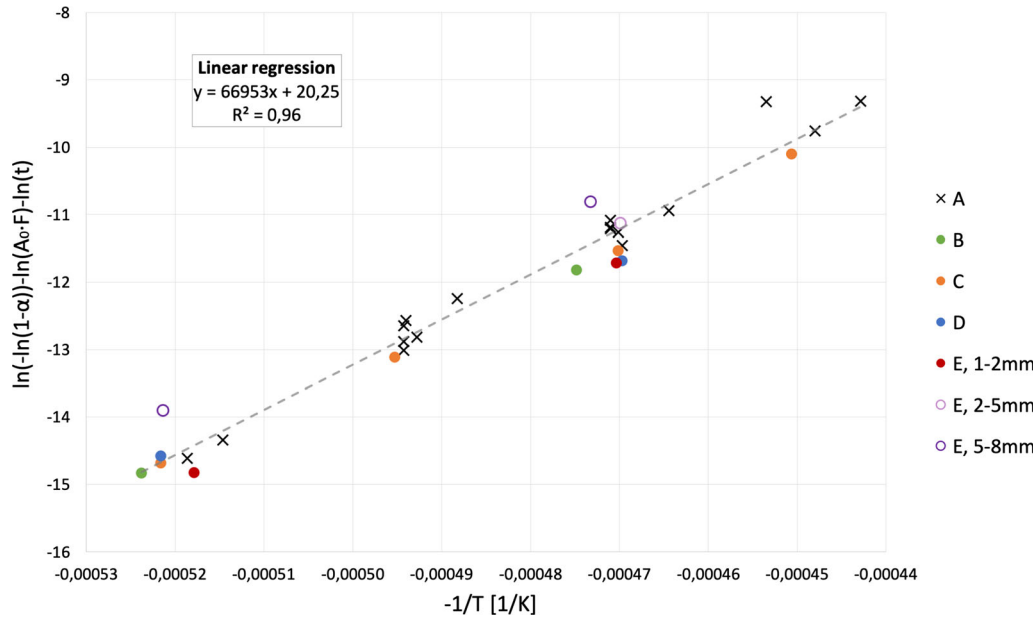| $k_0$ [g   s$^{-1}$ m$^{-2}$] | $Q$ [kJ mol$^{-1}$] |
| --- | --- |
| $6.2 \times 10^8$ | 557 |



Fig. 6—An Arrhenius plot of the experimental data. The different shapes (and colors) indicate the different types of quartz and the fraction of the raw materials in the case where different fractions were used for the same type of quartz (Color figure online).
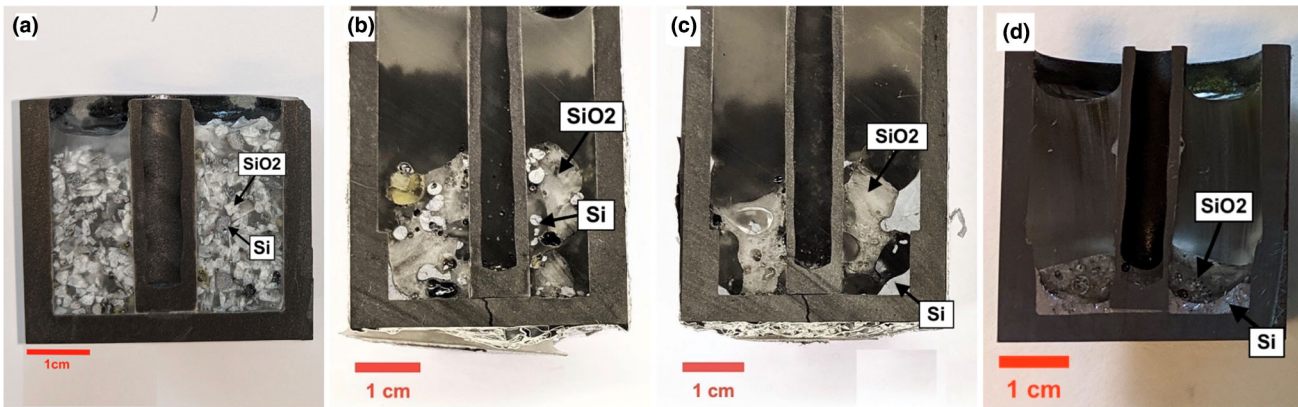


Fig. 7—The samples agglomerate as the degree of reaction ($\alpha$) increase. (a) 1650 °C for 120 min, $\alpha = 0.04$. (b) 1750 °C for 120 min, $\alpha = 0.09$. (c) 1850 °C for 60 min, $\alpha = 0.17$. (d) 1950 °C for 60 min, $\alpha = 0.56$.
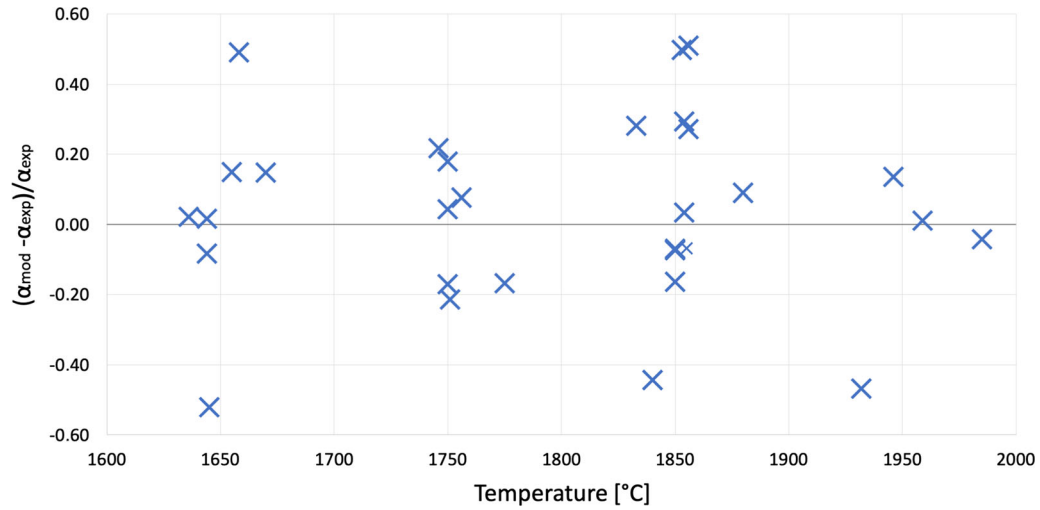
Fig. 8—The difference in modeled and experimental values for degree of reaction, relative to the experimental values, plotted as function of temperature.
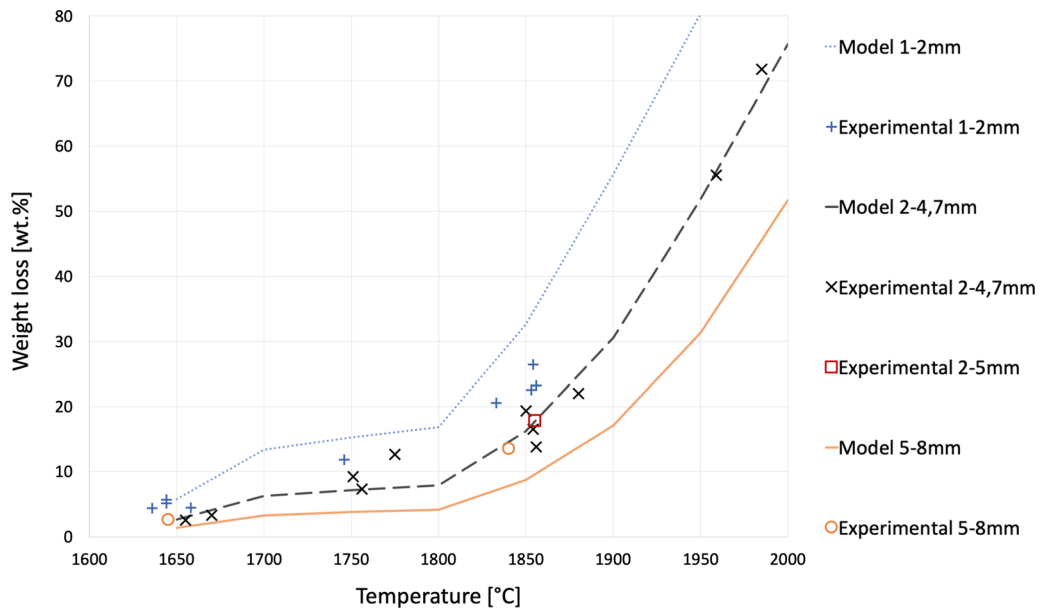


Fig. 9—The weight loss after heating samples to 1650 and 1750 °C for 120 min as well as 1850 and 1950 °C for 60 min. The size fraction of the samples and the modeled value for each fraction at the given time/temperature are additionally included.

The samples agglomerate as the temperature increase, as seen in Figure 7. This is included in the model as an agglomeration factor (F) which is part of the calculation of available reaction area, given by Eqs. [9] through [11]. Note that the agglomeration factor decreases as the degree of agglomeration increases. The degree of agglomeration is a function of temperature, but two constant values are chosen as agglomeration factor, to make the equation for reaction rate as simple as possible. Agglomeration is neglected below the melting point of quartz ($F = 1$) and the value above the melting point is chosen to be the value that give the best fit to experimental data ($F = 0.5$, indicating reduction in

available reaction area). There is not found any trend in error as function as temperature, as seen in Figure 8, which indicates that the chosen values for agglomeration factor is good. Silicon and silica were mixed before heating in most of the experiments, but some of the experiments with quartz A were performed with silicon layered on top of silica (see Table V for information on which samples that were mixed). There was no significant difference between the reaction rate of the samples that were mixed and the samples that were layered. The same equation for available reaction area is therefore used for both cases. Section "III−C" elaborates on the difference between layered and mixed samples.
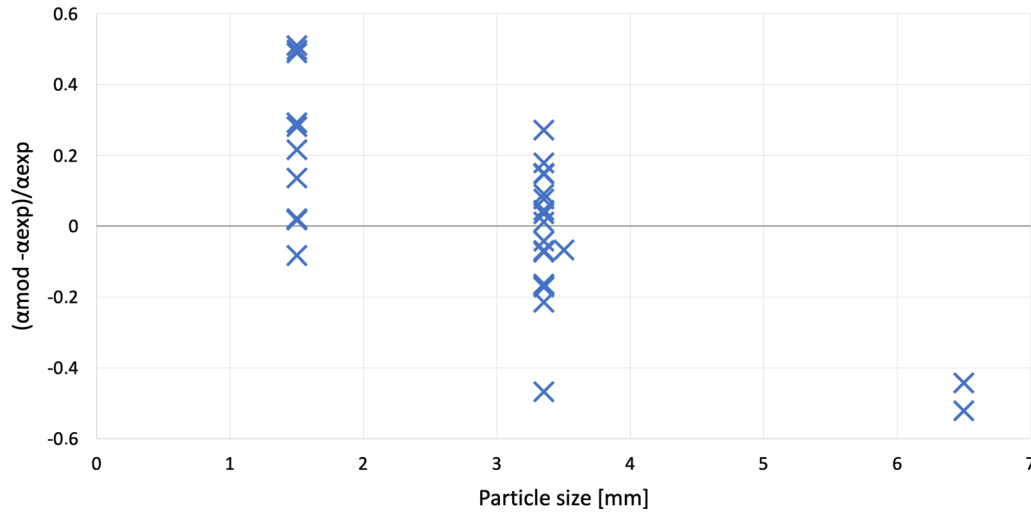
Fig. 10—The difference in modeled and experimental values for degree of reaction, relative to the experimental values, plotted as function of particle size.
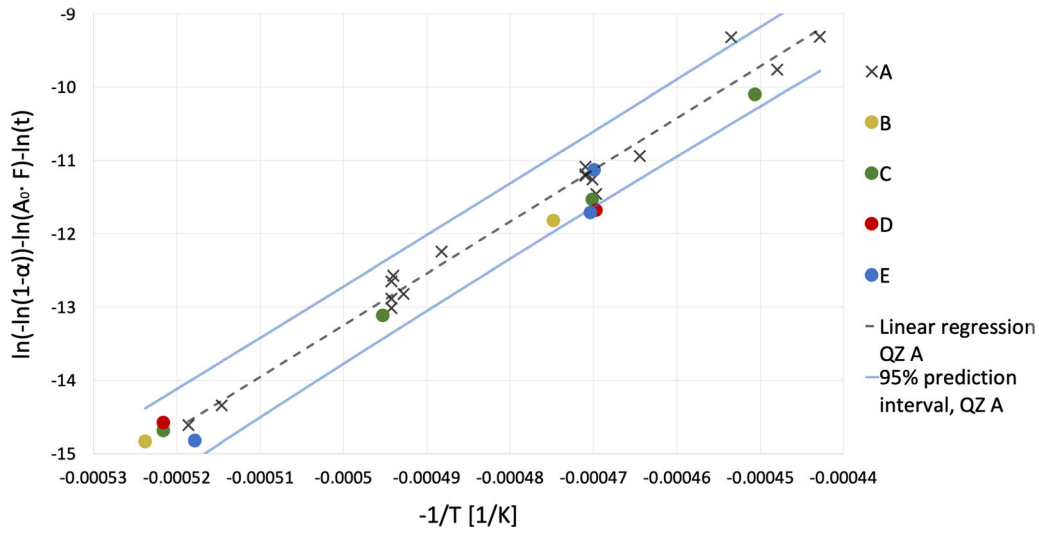


Fig. 11—An Arrhenius plot of all data points (except the two samples of 5 to 8 mm fraction) with linear regression and intervals based on quartz A only. All types of quartz seem to follow the same model.

$$\frac{d\alpha}{dt} = k_0 \, A \, \exp\left(-\frac{Q}{RT}\right) \qquad [8]$$

$$A = A_{0,Si} \, (1 - \alpha) \, F \qquad [9]$$

$$A_{0,Si} = \frac{1}{\rho_{Si}} \frac{S_{part.}}{V_{part.}} \qquad [10]$$

$$T < T_{m,QZ} \Rightarrow F = 1 \quad T > T_{m,QZ} \rightarrow F = 0.5 \qquad [11]$$

The data points from heating at 1650 °C and 1750 °C for 120 minutes and at 1850 °C and 1950 °C for 60 minutes have been selected and plotted along with a model for these times and temperatures, as shown in Figure 9. The model shows a good fit to the size fraction of 2 to 5 mm, but it predicts too high weight losses for samples of a smaller fraction and too low weight losses for samples of a higher fraction. This can also be seen in Figure 10 where the difference between the modeled and experimental values is plotted as a function of particle size. The trend in error indicates that there is a need for improvement in calculation of available area. Despite this, the model predicts reasonable values, and there is no trend in the error as function of temperature, as seen in Figure 8. This indicates that the value obtained for

activation energy is reasonable and it can be used for comparison of the different SiO-producing reactions in a silicon furnace.

## A. *The Reaction Rate of Different Industrial Quartz Samples*

Five different types of quartz have been included in the measurements of silicon/silica reaction rate. The amount of impurities in each quartz sample and their transformation rate vary significantly, but this does not seem to cause any significant difference in reaction rate. Figure 11 shows an Arrhenius plot of all reaction rate data obtained, except the two samples with a high fraction (5 to 8 mm). The figure includes a 95 pct prediction interval which is only based on data from heating of quartz A (the reference sample). One of the data points from quartz A lay outside the interval and two of the data points from quartz B to E lay at the border of the interval. It is therefore concluded that the reaction rate of silicon mixed with different types of quartz can be described by one equation. There is no significant difference between the reaction rate of the five different industrial quartz samples.

## B. *Formation of SiC at Crucible Interface*

In this work, the weight loss of a silicon and silica mixture is directly correlated to the degree of reaction; weight loss due to other reactions is neglected. A layer of silicon carbide was formed at the crucible interface of each sample, which is assumed to be due to reaction with both silicon and silica. Reaction with silica case would result in formation of CO gas in addition to SiO gas and the second case (reaction with silicon) would reduce the amount of silicon available for the $Si + SiO_2$ reaction. Both cases will affect the correlation between $Si/SiO_2$ reaction rate and weight loss of a $Si/SiO_2$ mixture heated in graphite crucibles. The layer thickness was measured at 13 samples and no correlation between the thickness, temperature, and time of the experiment was found. It is therefore assumed that a relatively dense and stable layer is formed after short time at low temperatures. Calculations were performed, to calculate an average weight loss of each sample, due to interaction with the crucible. The calculations were based on the assumption that the SiC layer is present on the inside of the graphite crucible up to a height of 2 cm, with a depth of 150 $\mu$m and that it is consisting of 75 vol pct graphite
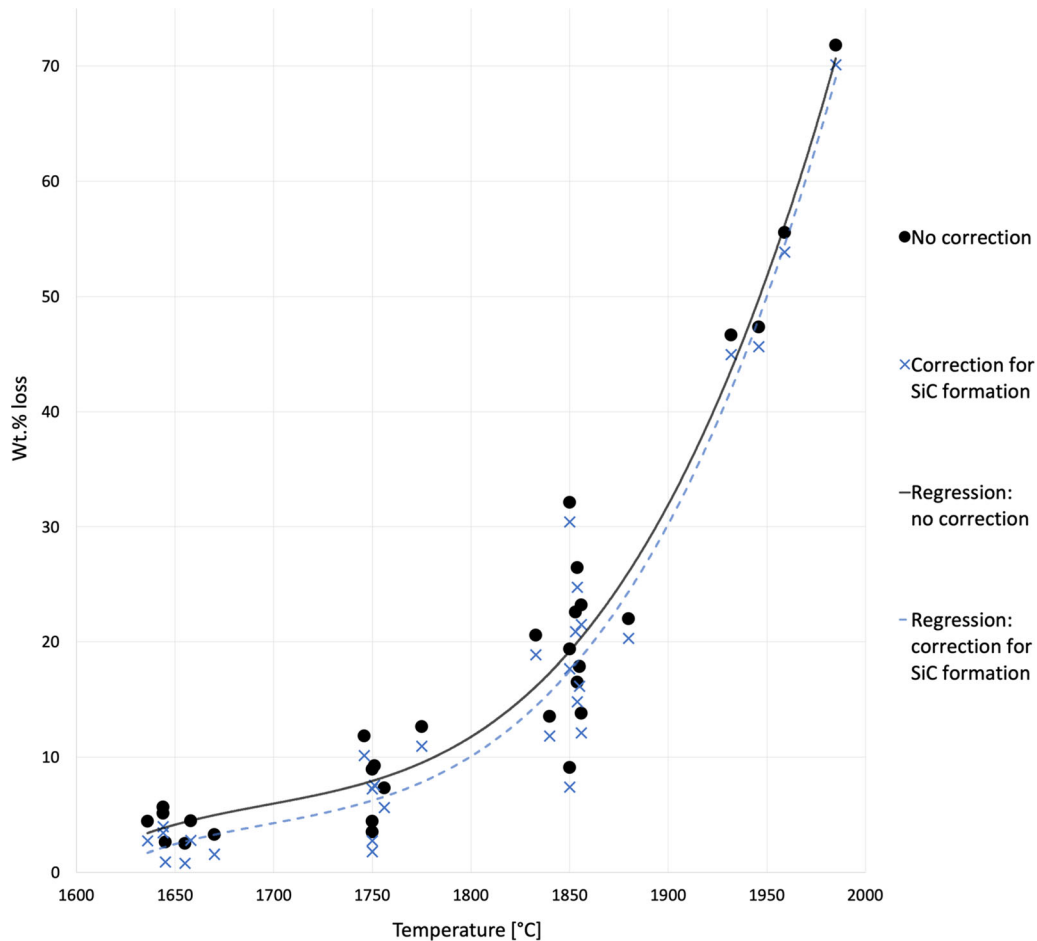


Fig. 12—The degree of reaction for each sample without any correction is plotted and marked with dots, while the degree of reaction with correction for weight loss due to SiC formation is marked with X's. The corrected value is based on total weight loss minus the weight loss due to interaction with crucible, causing formation of CO gas.
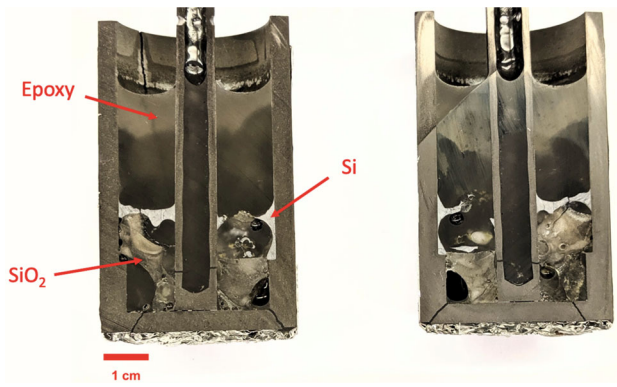
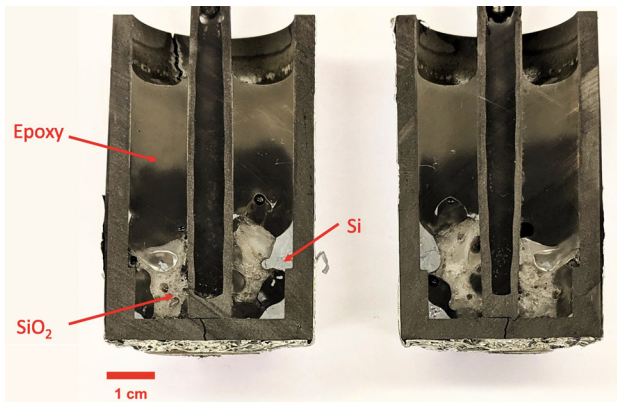Fig. 13—A sample heated for 60 min at 1850 °C. Mixed raw materials in a graphite crucible.



Fig. 15—A sample heated for 60 min at 1750 °C. Layered raw materials in a h-BN crucible.



Fig. 14—A sample heated for 60 min at 1850 °C. Layered raw materials in a graphite crucible.



Fig. 16—Image of a sample that was heated for 60 min at 1850 °C in a graphite crucible—picture taken with SEM BSE. The image is taken at the crucible interface, at a height where there is a small edge (the edge is not of importance to these experiments but could be used to separate crucible into two chambers). The image shows the expected phases, graphite (C), silicon carbide at the crucible interface, silica, and silicon with impurities at the grain boundaries. An approximate chemical composition at selected spots were obtained by EDS analysis.

and 25 vol pct SiC. Furthermore, it is assumed that 50 pct of the SiC was formed as a result of reaction with silica and the rest due to interaction with silicon. All of those assumptions are based on an average of values obtained by inspection of LOM and SEM images of 13 samples and the assumption that available reaction area is limiting both reactions (Si + C and $SiO_2$ + C). The last assumption is justified by values for Gibbs free energy listed in Table I, showing that both reactions can occur at temperatures above 1600 °C. Analysis of macro images shows that available reaction area is limited and within the same range for Si + C and $SiO_2$ + C.

This gave a total weight loss of 1.7 wt pct for each sample due to interaction with crucible, when the total sample weight is 20 g. This is a significant amount for samples heated to low temperatures, where the degree of reaction is low, but it is not significant for samples heated to higher temperatures. A plot of data for degree of reaction with and without a correction for formation of a SiC layer is included in Figure 12. Interaction with the crucible is still neglected in the entire temperature
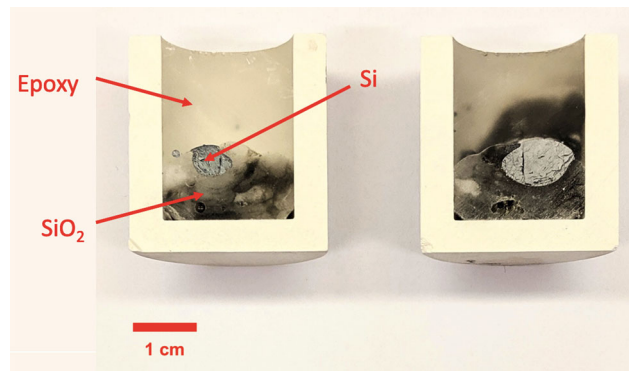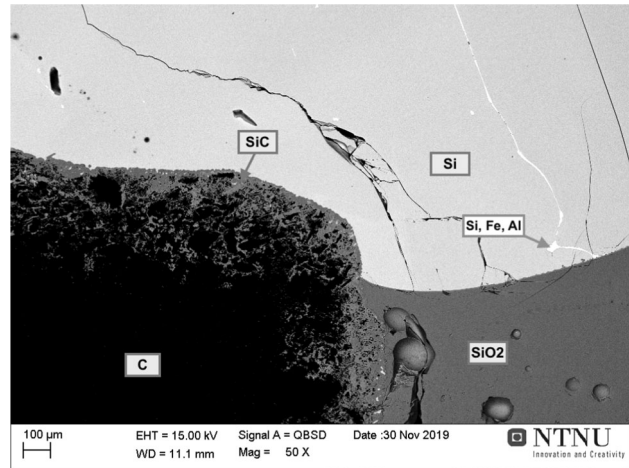
range of this model, to make the model as simple as possible, even though it is significant at 1650 °C. This means that the model might predict a reaction rate slightly too high at low temperature and time.

### C. Phase Distribution

Silicon and silica agglomerate at high temperature as shown in Figure 7. Both layering and mixing of silicon and silica have been performed prior to heating of the samples in a graphite crucible. Macro images of a sample where the raw materials were mixed before heating is shown in Figure 13 and an image from a sample where the raw materials were layered can be seen
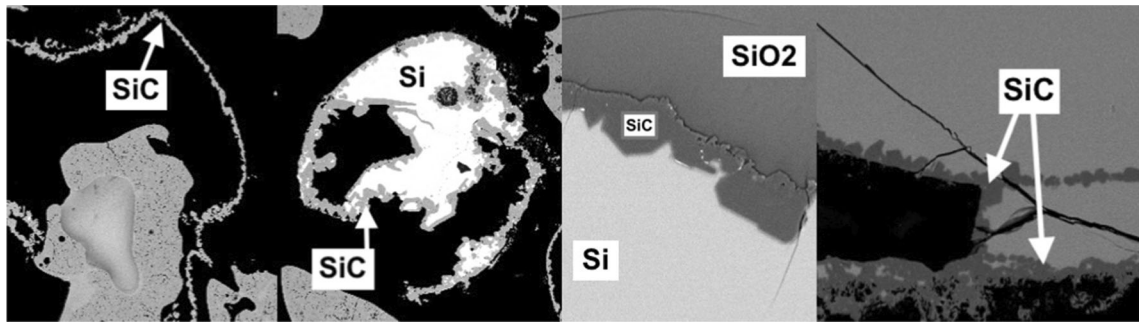
Fig. 17—Silicon carbide on the surface of silicon particles/droplets in samples heated to 1650 and 1750 °C.
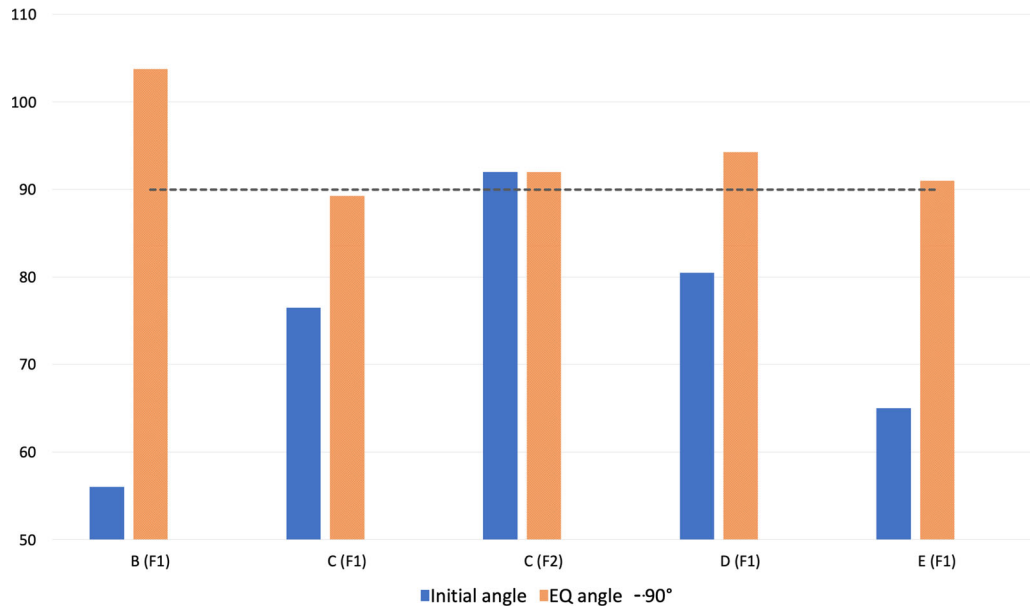


Fig. 18—The figure shows the initial wetting angle, right after complete melting and the equilibrium angle for silicon on substrates of quartz B to E. F1 indicates that furnace 1 was used, and F2 indicated that furnace 2 was used (two similar furnaces).

in Figure 14 (silicon layered on top of silica before heating). Silicon and silica agglomerate in both cases and the silicon tends to stay on top of the silica at temperatures up to 1900 °C, even though the density of silicon is higher than silica. There was not found any significant difference in the available reaction area for samples with layering and mixing of raw materials and whether the raw materials were mixed or layered did not affect the reaction rate significantly. One experiment was performed with heating of silicon and silica in a boron nitride crucible, to investigate the phase distribution after heating in a non-wetting crucible. The silicon did not drain to the bottom of the crucible in this case either, as seen in Figure 15. A high silica viscosity is therefore assumed to prevent the silicon from draining to the bottom of the crucible.

The samples were analyzed by SEM and the expected phases were found: Silicon, silica, graphite, and silicon carbide at the crucible interface, as seen in Figure 16. Furthermore, impurities at the grain boundaries of

silicon were found, which is expected, due to a low solubility of impurities in solid silicon. There was only one unexpected finding: Silicon carbide was found on the surface of the silicon heated to 1650 °C and 1750 °C, as seen in Figure 17; this was not found in samples heated to 1850 °C and 1950 °C. The reason for this is not fully understood, but an explanation could be that silicon carbide is formed at the surface of the silicon particles/droplets at low temperatures due to presence of small amounts of $CO_g$ ($\Delta G° < 0$ for $2Si + CO_g = SiO_{(g)} + SiC$ at $T < 1900°C$, according to values in Table I) and that the silicon carbide reacts with silica at higher temperature. This indicates that the silica/SiC reaction rate is low at temperatures up to 1750 °C, which is within agreement with work done by Tangstad et al.[3] The silicon carbide reduces the contact and reaction area between silicon and silica but there is still contact between the two phases due to the fact that the SiC layer has a low density. Empty shells of silicon carbide are observed, indicating that all of the silicon inside these
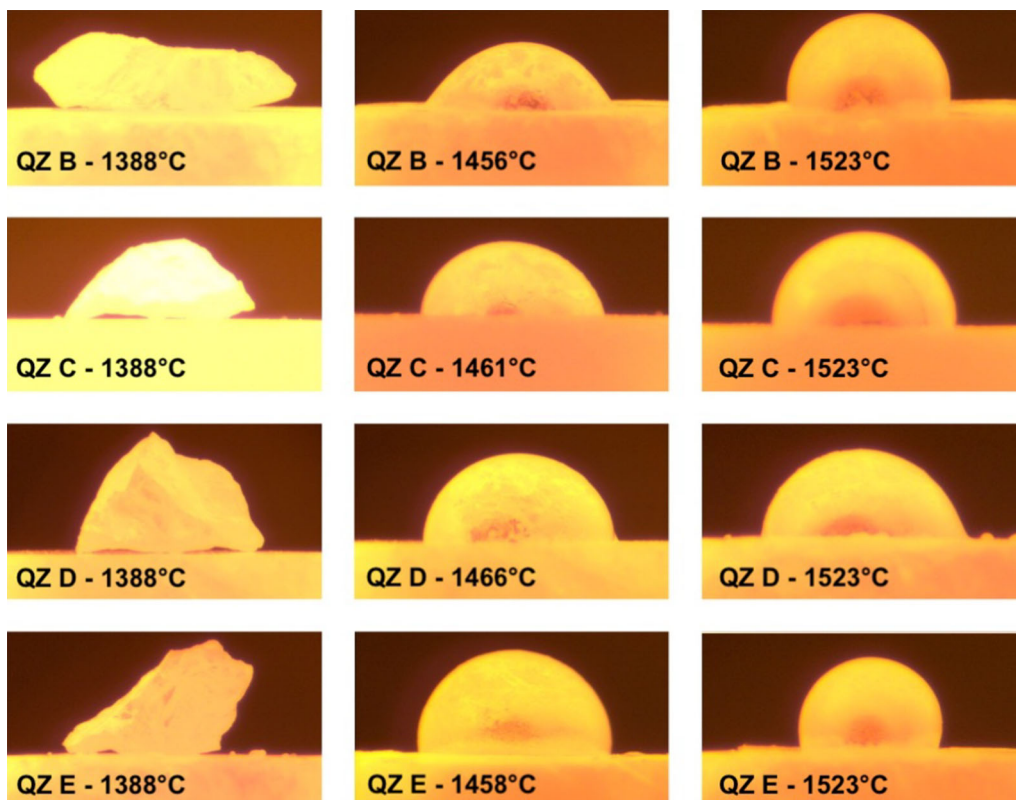
Fig. 19—Images taken during heating of the silicon and silica samples in furnace 1, one image of each quartz sample before the silicon melted (images to the left), one right after complete melting (images in the middle), and one image taken during the isothermal heat treatment at 1523 °C (images to the right). The type of quartz substrate and the temperature is indicated in each image.

droplets has reacted with silica. It is not known to what degree the silicon carbide layer affects the silicon/silica reaction rate and it is therefore not included in the model.

### D. Properties of the Different Quartz Samples

Silicon was heated on substrates of quartz B, C, D, and E in a sessile drop furnace, to investigate the silicon/quartz wettability. The initial angle was right below 90° for all, except for one parallel of sample C which was measured in a different, but similar furnace. The formation of bubbles at the silicon/silica interface starts right after melting of the silicon, which is assumed to be formation of SiO gas. The wetting angle starts to increase at the same time, up to 89 to 94 deg for all samples except for quartz B which increases to 104 °C. The wetting angle increases for a few minutes and reaches an equilibrium before the isothermal temperature of 1523 °C is reached. The equilibrium angle is reached a short time after melting and is therefore assumed to be the angle of importance, both in the experiments performed in this work and for behavior in an industrial furnace. The wetting angle oscillates with a few degrees at equilibrium, most likely due to gas formation at the silicon/silica interface, but it is kept above 90 °C for all samples (except one parallel of

quartz C that oscillated around 89 °C). It is therefore concluded that silicon does not wet either of the industrial quartz samples and the wetting angle ranges from 90 to 95 °C, except quartz B who has a wetting angle in the range of 100 to 110 °C, as shown in Figure 18. Images of the samples before melting, right after melting and at equilibrium, can be found in Figure 19. It should be noted that quartz B is the sample with the lowest impurity content. Literature reports a wetting angle between silicon and pure silica of 90 °C to 95 °C , which is coherent with the measured wetting angle for silicon on substrates of quartz C to E.

All of the quartz samples (A to E) were heated to 1650 °C in alumina crucibles and held for 120 minutes before being cooled and analyzed by XRD, to investigate the phase distribution in each sample. There was no significant difference between the phase composition of the samples after heating, except quartz E which had a higher amount of amorphous phase. All types of quartz will transform to cristobalite at 1650 °C after enough time. It seems like the chosen holding time of 120 minutes (corresponding to the holding time used for silicon/silica samples heated to 1650 °C) is long enough for all the samples to approach equilibrium phase composition. However, as stated by Jusnes, there is a significant difference in transformation rate of quartz B,
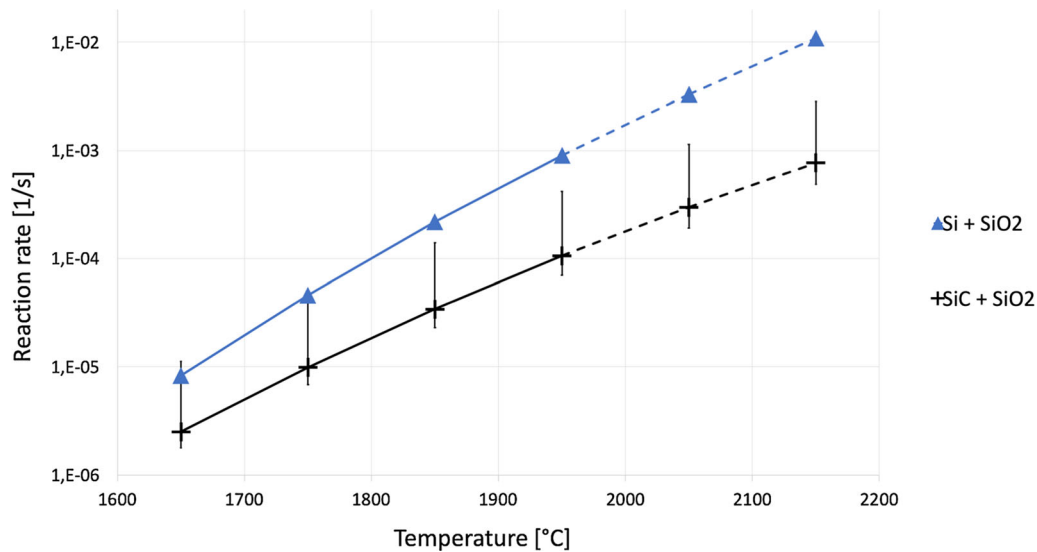
Fig. 20—The reaction rate of the two SiO-producing reactions in a silicon furnace for a given reaction area on a logarithmic scale. The reaction area (A) is set to be determined by 1 to 2 mm silicon particles for the silicon/silica reaction and 1 to 2 mm silica particles for the silica/SiC reaction (marked by crosses). The reaction rate for $SiO_2$ + SiC was obtained from a model developed by Tangstad et al. (marked by triangles).[3] The reaction rate for $SiO_2$/Si was obtained by the model developed in this thesis. The dotted line is outside the temperature range of the models.

C, and D (the work does not include quartz A and E).[9] Hence, it can be concluded that the transformation rate does not affect the SiO formation of the silicon/silica mixtures in this report. This could be due to the fact that most of the samples were heated at higher temperatures when silicon/silica reaction rate was measured, at temperatures where all of the samples will be transformed into cristobalite and start melting before the isothermal temperature is reached.

The work done by Jusnes et al. shows that there is a significant difference in decrepitation of quartz B, C, and D after shock heating. [12] Decrepitation after shock heating does not seem to affect reaction rate of silicon and silica mixtures, because the samples have a difference in decrepitation but no difference was found in their reaction rate. The samples were heated at a rate of 50 °C/min in the experiments where the reaction rate was measured, and one can assume that decrepitation might affect reaction rate of a mixture if the samples are shock heated. The surface of silicon is lower than the surface of silica in the experiments where weight loss of a 1:1 molar mixture is measured, due to a density difference. Any agglomeration of the silicon and decrepitation of the quartz would further reduce the surface area of silicon relative to the silica. This verifies that the surface area of silicon is the limiting factor when it comes to available reaction area, and it is a good assumption for available reaction area, as used in this reaction model, $A_{0,model} = A_{0,Si}$.

There is a significant difference in the melting rate of quartz B and C but no information has been obtained for the other samples. The melting rate of each quartz sample is however assumed to be quite different in the present experiments, due to a large difference observed between quartz B, C, and other industrial samples.[11] As this has not affected the reaction rate between silicon and silica, this verifies that the overall reaction rate is independent on the melting rate. It should however be noted that the experiments have been performed at 1650 °C, 1750 °C, 1850 °C, and 1950 °C, at relatively large temperature intervals and there might be a local variation in reaction rate due to a difference in melting rate.

There is a significant difference in content of impurities, decrepitation after shock heating, and rate of phase transformation between the different types of quartz, but no significant difference in reaction rate. Therefore, it is assumed that impurities, decrepitation after shock heating, and phase transformation rate have an insignificant impact on the reaction rate of silicon and silica mixtures when heated at a rate of 19 °C/min. There is a significant difference in melting rate of each sample and it is assumed to not affect the overall reaction rate, but there could be local differences between the different quartz samples in the temperature range where the samples soften and melt.

### E. Comparison of the Two SiO-Producing Reactions in a Silicon Furnace

Figure 20 shows the reaction rate of both SiO-producing reactions on a logarithmic scale, in a temperature range from 1650 to 2150 °C. The figure is based on an initial reaction rate for the $Si/SiO_2$ and $SiC/SiO_2$ reaction described by Eqs. [8] through [5], respectively. The initial reaction area ($A_0$) is set to be 17.4 cm$^2$ g$_{Si}^{-1}$ for the silica/silicon reaction and 15.1 cm$^2$ g$_{SiO_2}^{-1}$ for the silica/SiC reaction. This is based on calculation of available reaction area for the two reactions, where 1 to 2 mm particles of silicon limit the reaction rate of Si/$SiO_2$ and 1 to 2 mm particles of $SiO_2$ limit the reaction rate of $SiO_2$/SiC. The calculation of initial reaction area is described by Eq. [10] for the silicon/silica reaction and the same calculations have been performed for the silica/

silicon carbide reaction, where the density of silicon was replaced by density of silica. The black line in Figure 20 represents the reaction rate of silicon and silicon carbide based on the average activation energy and the error bars indicate rate based on maximum and minimum values reported by Tangstad et al.[3]

There is a difference between the reaction rate of the two reactions in this case, as seen in Figure 20. The difference is small at low temperatures, but significant at higher temperatures. Therefore, it could be argued that there is a significant difference between the rate of each reaction at elevated temperatures for the given available reaction area, but the reaction rate of both reactions is highly dependent on the available reaction area. The available reaction area could vary significantly for the two SiO-producing reactions within a furnace. This leads to the conclusion that the production of SiO gas in a silicon furnace is highly dependent on the available reaction area for the two possible reactions.

## IV. CONCLUSION

The reaction rate of a silicon and silica mixture increases with time and temperature and can be described by Eq. [12] for various types of industrial quartz. The reaction $Si + SiO_2$ has a reaction constant ($k_0$) equal to $6.25 \times 10^8$ g s$^{-1}$ m$^2$ and an activation energy ($Q$) equal to 557 kJ mol$^{-1}$. Impurities, decrepitation after shock heating, melting rate, and phase transformation rate are silica properties that have an insignificant impact on the reaction rate of silicon and silica mixtures when heated at a rate of 50 °C/min.

$$\frac{\mathrm{d}\alpha}{\mathrm{d}t} = 6.25 \times 10^8\, A \, \exp\left(-\frac{557\,10^3}{RT}\right). \qquad [12]$$

The reaction rate of the two SiO-producing reactions in a silicon furnace ($Si + SiO_2$ and $SiO_2 + SiC$) is within the same range as long as their available reaction area is within the same range. The reaction rate of both reactions increases significantly with temperature and so does their available reaction area as you go deeper in a silicon furnace. This means that whether reaction with silicon or silicon carbide contributes the most towards formation of SiO gas in a silicon furnace is determined by the phase distribution in the hot-temperature zone.

The calculation of available reaction area is one weakness of this model. There is a trend in the difference between experimental data and modeled data as a function of particle size. This indicates that the expression for available reaction area could be improved. The reaction rate of silicon and silica is shown to increase with time and temperature, but work done by Andersen indicates that there might be a local reduction of rate around the melting point of silica.[5] Whether there is a local drop or not could be verified by a few experiments at temperatures ranging from 1700 to 1750 °C. Despite that, the model is considered to predict reasonable values for reaction rate of a silicon and silica mixture in the range from 1650 to 1950 °C.

## REFERENCES

1. A. Schei, J.K. Tuset, and H. Tveit: *Production of High Silicon Alloys*, Tapir, Trondheim, 1998.
2. F. Li and M. Tangstad: *Metall. Trans. B*, 2017, vol. 48, p. 853.
3. M. Tangstad, J. Safarian, S. Bao, E. Ringdalen, and A. Valderhaug: *Aspects Min. Miner. Sci.*, 2019, vol. 3, p. 2.
4. S. Bao, M. Tangstad, K. Tang, E. Ringdalen, The thirteenth International Ferroalloys Congress - Efficient technologies in ferroalloy industry 273–282 (2013).
5. V. Andersen, Condensate formation in the silicon process. Master's thesis, Norwegian University of Science and Technology (2011).
6. C. Klein and C.S. Hurlbut: *Manual of Mineralogy*, 21th ed., Wiley, New York, 1993.
7. G. Blackman: *Si Chemical Data*, 7th ed., Wiley, New York, 2014.
8. S.J. Stevens, R.J. Hand, and J.H. Sharp: *J. Mater. Sci.*, 1997, vol. 32, p. 2929.
9. K. Jusnes, Phase transformations and thermal degradation in industrial quartz. Ph.D. thesis, Norwegian University of Science and Technology (2020).
10. M.E. Kjelstadli, Kinetics and mechanism of phase transformations from quartz to cristobalite. Master's thesis, Norwegian University of Science and Technology (2016).
11. E. Nordnes, Softening and melting properties of quartz. Master's thesis, Norwegian University of Science and Technology (2019).
12. K.F. Jusnes, M. Tangstad, E. Ringdalen, in *Infacon XV: International Ferro-Alloys Congress, Cape Town, South Africa*, ed. by R. Jones, P. den Hoed (2018).
13. A. Ciftja, T.A. Engh, and M. Tangstad: *Metall. Trans. B*, 2010, vol. 41, pp. 3183–95.
14. O. Dezellus, S. Jacques, F. Hodaj, and N. Eustathopoulos: *J. Mater. Sci.*, 2005, vol. 40, pp. 2307–11.

15. L.D. Alphei, R. Grotjahn, V. Becker, R. Janhsen, M. Douvidzon, and J.A. Becker: *J. Mater. Sci.*, 2013, vol. 48, p. 7350.
16. H. Kanai, S. Sugihara, H. Yamaguchi, T. Uchimaru, N. Obata, T. Kikuchi, F. Kimura, and M. Ichinokura: *J. Mater. Sci.*, 2007, vol. 42, p. 9529.
17. H. Fujii, M. Yamamoto, S. Hara, and K. Nogi: *J. Mater. Sci.*, 1999, vol. 34, p. 3165.
18. J. Vangskåsen, Condensate formation in the silicon process. Master's thesis, Norwegian University of Science and Technology (2011).
19. B. Drevet, R. Voytovych, R. Israel, and N. Eustathopoulos: *J. Eur. Ceram. Soc.*, 2009, vol. 29, p. 2263.
20. Z. Yuan, W.L. Huang, and K. Mukai: *Appl. Phys. A*, 2004, vol. 78, p. 617.
21. J.A. Champion, B.J. keene, and S. Allen: *J. Mater. Sci.*, 1973, vol. 8, p. 423.